Title:
Developing Geometric Analysis Tools to Compare Heat Map Results for Metal Additive Manufactured Components

Authors:
Ruth Jill Urbanic, jurbanic@uwindsor.ca, University of Windsor
Bita Mohajernia, mohajerb@uwindsor.ca, University of Windsor
Navid Nazemi, navid.nazemi@aecom.com, AECOM

Keywords:
Metal Additive Manufacturing, Finite Element Modeling Geometric Based Interpretation, Physical Properties, Residual Stress, Comparative methods

DOI: 10.14733/cadconfP.2019.164-168

Introduction:
Laser cladding is usually utilized for coating surfaces to improve the performance of the surface (corrosion or wear resistance) or to repair it if it is worn. This process has evolved into a viable metal additive manufacturing (AM) solution, and is termed the direct energy deposition (DED) AM process. In this process, a laser beam melts the material powder flowing from a nozzle while it is being distributed onto a surface. A thin layer on the surface of the substrate melts to help forming a bond between the clad material and the substrate material. A shielding gas such as argon protects the melt pool from the atmosphere to prevent oxidization. The DED input parameters play a significant role in the quality of the bead [3, 4, 6], the dilution zone (the region where the substrate and deposition materials mix), and the heat affected zone (HAZ) (shown in Fig. 1), as well as the bead geometry [1, 2, 5]. As a result, understanding the influence of the input parameters on the resulting mechanical and physical properties is a concern for both equipment manufacturers, and process planners or fabricators.

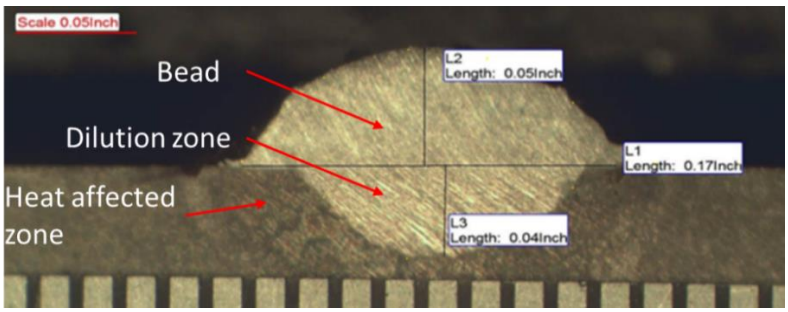

Fig. 1: A single laser clad bead, showing the dilution and heat affected zones (with 0.2 mm gradients).

Each input parameter (laser power, travel speed, powder feed rate, contact tip to work piece distance) has a distinct effect on the bead's mechanical and physical properties. It is crucial to find the best combination of input parameters to deposit a bead with the desired geometry and mechanical properties. The generation of residual stresses due to the high thermal gradients, and the non- uniform plastic deformation of the base substrate or plate, are two of the most important issues when analyzing

the mechanical properties of the bead. Residual stresses can lead to undesirable distortion and cracks; therefore, (i) understanding the residual stress characteristics, (ii) linking them to the bead geometry and input parameters, and (iii) developing predictive models are active areas of research. Item (i) is addressed by conducting experimentally calibrated finite element analyses to provide insights; however, items (ii) and (iii) have significant research challenges, as the induced residual stresses (or hardness) are not discrete values such as the bead geometry shape characteristics.

Prior AM DED research has been conducted utilizing P420 stainless steel as the clad material and AISI 1018 steel as the substrate material and a 4kW diode laser-robotic cell configuration. The process parameters, factor levels for the design of experiments, and their corresponding values are presented in Tab. 1. The bead geometry for experiment A and B, and residual stress levels in the bead center are illustrated in Fig. 2. The residual stress measurement was conducted using the Proto X-ray diffraction system (Lab 002/LXRD 06024) [8] for two samples in the 'as clad' and 'heat treated' states. The operating parameters for the measurements are presented in Tab. 2. Six subsurface measurements were done – 0 represents the top of the bead. The upper and lower bounds (red dashed lines) are calculated from the collected data using a 90% confidence interval and used as a basis to assess the goodness of the developed finite element model. The developed FEA model (using SYSWELD [9]) and the experimental results are presented for the non-heat treated (NHT) results in Fig. 2. The FEA results correlate well to the experimental data. For a complete description of the model and mesh development, validation, experimental configuration and results, please refer to Nazemi and Urbanic [7].

Parameters	*Factor levels*				
	-2	-1	0	1	2
Powder feed rate (gr/min)	10	***15***	**20**	25	30
Laser power (kW)	1	***2***	**2.5**	3	4
Focal length of lens (mm)	380	***390***	**400**	410	420
Laser speed (mm/s)	5	***7.5***	**10**	12.5	15
Contact tip to work piece distance (mm)	**21**	22	23	***24***	25

Tab. 1: Single bead experimental configuration, with the bolded text highlighting the process parameters for experiment A, and the red *italicized* text highlighting the process parameters for experiment B.

X-Ray Elastic Constant	*Crystallographic Plane*	*Brag angle*	*Gain Material*	*Aperture*	*Oscillation(s)*	*Collection Time*
25578.95 ksi	{211}	155.1˚	Titanium - Beta	1.0 mm - round	Beta 4.0 ˚	4 minutes

Tab. 2: X-ray diffraction parameters.

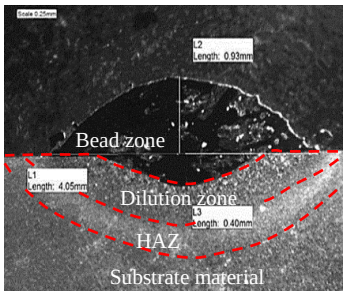

(a)
Width = 4.05 mm
Height = 0.93 mm
Depth = 0.40 mm

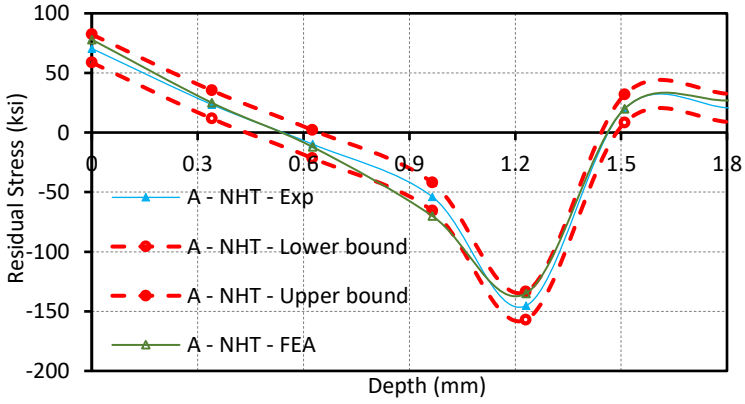

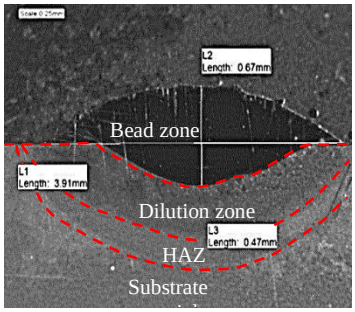

(b)
Width = 3.91 mm
Height = 0.67 mm
Depth = 0.47 mm

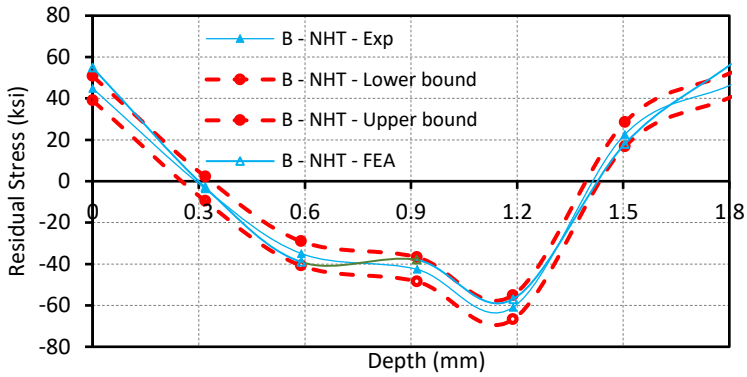

Fig. 2: A single laser clad bead, showing the dilution and heat affected zones.

The results from the complete simulation model can be analysed in regions of interest (Fig. 3). Extending the model to analyze multiple beads with differing overlap and process configurations has been done; however, the research question focuses on how to comprehensively compare results quantitatively, and develop a predictive model that will encompass both the bead geometry and physical properties. The goal of this research is to transform the mechanical or physical property heat maps, or isoline representations, for process build configurations into geometric data, which is turn can be used to seed an artificial neural network predictive model.

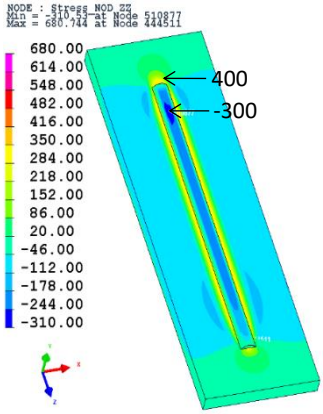

(a)

(b)

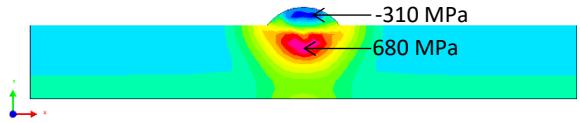

Fig. 3: (a) Longitudinal residual stress contours for specimen *A* from the simulation (b) cross-section view (specimen center).

Main Idea:
The induced residual stress magnitudes and patterns will vary based on the input parameters and the bead overlap percentage. Finite element model results are derived for 9 configurations, which are presented in Tab. 3, and sample results are illustrated in Fig. 4. It is readily evident that the magnitudes and positions of the stress regions vary. An effective predictive model cannot focus on absolute maximum and minimum stress magnitudes, but must include intermediate values and their positions. Therefore, a standardized method for direct comparisons needs to be determined for any *x,y,z* coordinate, as well as the observed residual stress patterns. It is proposed to convert the results models into topology via contour extraction and solid modeling tools to extract residual stress values (and changes in residual stress) patterns as well as creating medial lines that could be used for pattern recognition purposes. This data will be used as an input for artificial neural network models.

40%, 50%, 60% overlap	*A*	*B*	*C*
Powder feed rate (g/min)	20	20	20
Laser power (KW)	2.5	2.5	2
Focal length of lens (mm)	400	400	400
Laser speed (mm/S)	10	12	12

Tab. 3: Multi-bead process parameters and overlap configurations used for the FEA models.

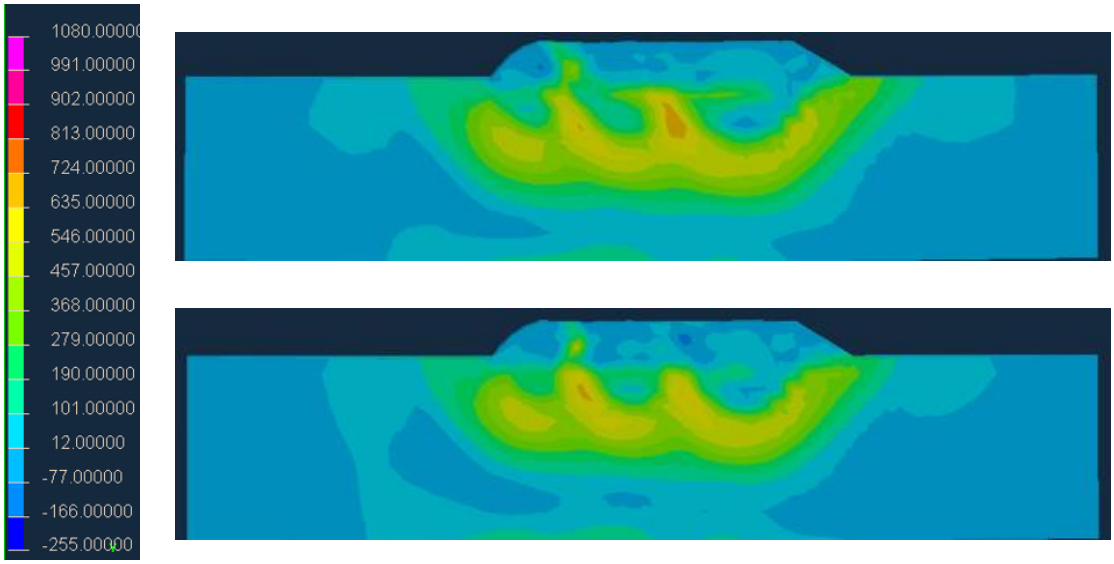

Fig. 4: Residual stress scale, and the results for 40% overlap for experiment A (top) and C (bottom).

Topology creation solutions in Rhino© (or other image to CAD conversion software tools) do not isolate each bounded region well. The methodology and tools for proposed here are:

- Employ a common scale for the iso curves / heat map colors and the FEA model geometry
- Extract the boundary contours (GIMP) for the heat maps (Fig. 5 (a) and (b))
- Create NURB curves (Mastercam) from the boundary curves (isolines or GIMP solution)
- Create solid models of the regions, where each solid model color correlates to a stress, and compare the models developed from the various process configurations (Mastercam) (Fig. 5 (c)).
- Create Voronoi diagrams, and extract medial lines from the boundary curves and compare results (Rhino© and Grasshopper© tools) (Fig. 5 (d)).

The boundary curves created from an image may have some noise as shown in Fig. 5 top; consequently, a filtering configuration needs to be established. However, once the geometry is created, detailed analytical comparisons can be performed. With a unit extrusion height, the size and centers of each stress region can be determined using standard solid model analysis tools, and correlated to the bead geometry. Employing a unique height for each solid region and trimming the geometry at selected planes will allow for users to create residual stress and residual stress rate change profile curves with respect to the desired Cartesian coordinates, which can be used to seed a black box predictive modeling solution.

Conclusions:

Advanced FE models, which include thermal-metallurgical-mechanical characteristics, can effectively simulate mechanical and physical properties for the AM DED process, such as the residual stresses induced due to the aggressive thermal cycling. However, there are challenges related to comparing results at a detailed, systematic level. Hence, it is proposed to translate the FE model results into geometry that can be employed for comparisons and developing predictive models. The procedures

need to be finalized, and then automated. Results for different approaches will be presented in the paper.

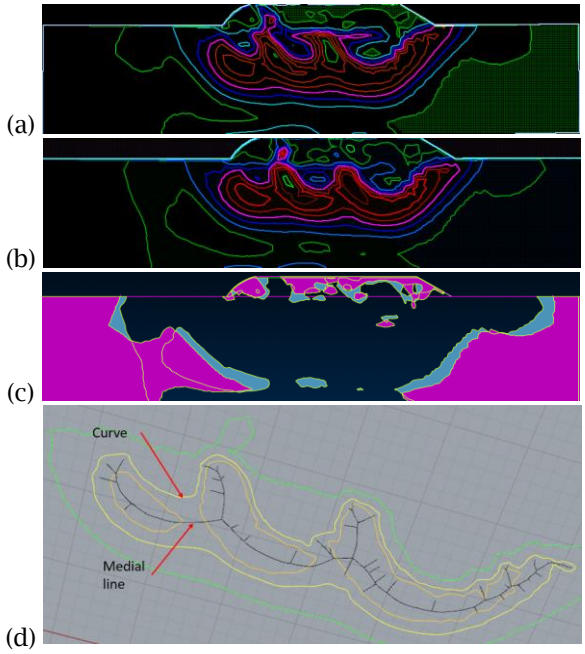

Fig. 5: Residual stress boundary curves for the 40% overlap for experiment A (a) and C (b), and boundary curves solid model overlay for the low stress regions (c), and medial line for the selected curve (d).

References:

[1] Aggarwal, K.; Urbanic, R. J.; Saqib, S.: Development of predictive models for effective process parameter selection for single and overlapping laser clad bead geometry, Rapid Prototyping Journal, 24(1), 2018, 214-228. https://doi.org/10.1108/RPJ-04-2016-0059
[2] El-Cheikh. H.; Courant, B.; Branchu, S.; Hascoet, J.; Guillen. R.: Analysis and prediction of single laser tracks geometrical characteristics in coaxial laser cladding process, Optics and Lasers in Engineering. 50(3), 2012, 413-422. https://doi.org/10.1016/j.optlaseng.2011.10.014
[3] Chew, Y.; Pang, J.; Bi, G.; Song, B.: Thermo-mechanical model for simulating laser cladding induced residual stresses with single and multiple clad beads, Journal of Materials Processing Technology, 224, 2015, 89-101. https://doi.org/10.1016/j.jmatprotec.2015.04.031
[4] Farahmand, P.; Kovacevic, R.: An experimental-numerical investigation of heat distribution and stress field in single- and multi-track laser cladding by a high-power direct diode laser, Optics & Laser Technology, 63, 2014, 154-168. https://doi.org/10.1016/j.optlastec.2014.04.016
[5] Goodarzi, D.; Pekkarinen, J.; Salminen, A.: Analysis of laser cladding process parameter influence on the clad bead geometry, Welding in the World, 61(5), 2017, 883–891. https://doi.org/10.1007/s40194-017-0495-0
[6] Nazemi, N.; Urbanic, R. J.: A numerical investigation for alternative toolpath deposition solutions for surface cladding of stainless steel P420 powder on AISI 1018 steel substrate, International Journal of Advanced Manufacturing Technology, 96/(9-12), 2018, 4123-4143. https://doi.org/10.1007/s00170-018-1840-1
[7] Nazemi, N.; Urbanic, R. J.; Alam, M.: Hardness and residual stress modeling of powder injection laser cladding of P420 coating on AISI 1018 substrate, International Journal of Advanced Manufacturing Technololgy, 93, 2017, 3485. https://doi.org/10.1007/s00170-017-0760-9
[8] Proto Manufacturing https://www.protoxrd.com/
[9] SYSWELD: ESI-Group (2015) SYSWELD 2015 reference manual